A First-Principles Study on Electron Donor and Acceptor Molecules Adsorbed on Phosphorene

ARTICLE *in* THE JOURNAL OF PHYSICAL CHEMISTRY C · JANUARY 2015

Impact Factor: 4.77 · DOI: 10.1021/jp5116564

3 AUTHORS, INCLUDING:

Ruiqi Zhang
University of Science and Technology of China
5 PUBLICATIONS **11** CITATIONS
SEE PROFILE

Jinlong Yang
University of Science and Technology of China
510 PUBLICATIONS **11,091** CITATIONS
SEE PROFILE

THE JOURNAL OF PHYSICAL CHEMISTRY C

Article

pubs.acs.org/JPCC

A First-Principles Study on Electron Donor and Acceptor Molecules Adsorbed on Phosphorene

Ruiqi Zhang,[†] Bin Li,*[,†,‡] and Jinlong Yang*[,†,‡]

[†]Hefei National Laboratory for Physics at Microscale and [‡]Synergetic Innovation Center of Quantum Information & Quantum Physics, University of Science and Technology of China, Hefei, Anhui 230026, China

ABSTRACT: Density functional theory calculations have been carried out to investigate single-layer phosphorene functionalized with two kinds of organic molecules, i.e., an electrophilic molecule tetracyano-*p*-quinodimethane (TCNQ) as electron acceptor and a nucleophilic molecule tetrathiafulvalene (TTF) as electron donor. The TCNQ molecule introduces shallow acceptor states in the gap of phosphorene close to the valence band edge, which makes the doped system become a p-type semiconductor. However, when the TTF molecule is adsorbed on the phosphorene, the occupied molecular states introduced into the gap are of deep donor states so that effective n-doping for transport cannot be realized. This disadvantageous situation can be amended by applying an external out-of-plane electric field with direction from phosphorene to TTF, or an in-plane tensile strain, or their combination, under which the conduction band edge of the phosphorene moves closer to the TTF-derived donor states, and then the TTF-adsorbed phosphorene system becomes an n-type semiconductor. It is also noted that the out-of-plane electric field and in-plane strain can modulate the band gap of the TTF-adsorbed phosphorene markedly. The effective bipolar doping of single-layer phosphorene via molecular adsorption, especially n-doping against its native p-doping propensity, and the good response of band gap in the infrared waveband of the TTF-adsorbed phosphorene to the out-of-plane electric field and in-plane strain would broaden the way to the application of this new type of two-dimensional material in nanoelectronic and optoelectronic devices.

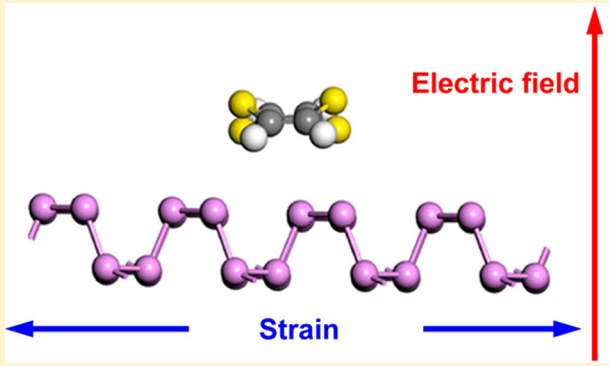

I. INTRODUCTION

In recent years, graphene-like two-dimensional (2D) materials, owing to their remarkable properties,[1,2] have attracted much research attention as emerging device materials for nanoelectronics. These materials, such as graphene,[3,4] silicene,[5−7] boron nitride nanosheets,[8−10] and 2D transition-metal dichalcogenides (TMDs),[11] have novel properties which are different from their bulk counterparts. With many promising applications in nanoelectronics and optoelectronics, the 2D materials are considered to be a relatively new and exciting area for nanotechnology.

Recently, a new 2D semiconducting material, namely, few-layer black phosphorus or phosphorene, has been isolated successfully by mechanical exfoliation from black phosphorus crystals.[12,13] Unlike the widely studied other 2D materials, phosphorene exhibits a sizable and novel direct band gap, which can be modified from 1.51 eV for a monolayer to 0.59 eV for a five-layer.[14] Besides, the phosphorene-based field-effect transistor (FET) exhibits high mobility of 286 $cm^2/(V\ s)$, and phosphorene possesses highly on/off ratios, up to 10^4 mobility.[10] With some other interesting and useful features, such as its anisotropic electric conductance and optical responses, phosphorene is considered to be a remarkable 2D material for electronic and optical applications[15] and has immediately received considerable research attention.[16−18]

On the basis of our current understanding, well-behaved p-type FETs based on few-layer phosphorene[12,14] and black phosphorus monolayer MoS_2 van der Waals heterojunction p−n diode were fabricated in recent experiments.[19] The p-type conductivity observed in these experiments of the phosphorene sample was attributed to intrinsic point defect states of the phosphorene.[20] It is well-known that many electronic devices, such as p−n junctions and complementary metal oxide semiconductors (CMOS), require ability of the semiconductor to be both p-doped and n-doped. Especially, the effective n-type doping of phosphorene is important because of its native p-type doping property. It is necessary to employ specific methods to modulate electronic structure of the phosphorene so as to make this new 2D material suitable to broader applications.

Molecular doping is a promising, simple, and effective way to tune the electronic structures of 2D materials via their interactions with the molecule because a large variety of inorganic and organic molecules are available. Especially, a lot of the organic molecules have been designed and synthesized, and different functional groups can be incorporated into them

Received: November 21, 2014
Revised: December 31, 2014
Published: January 14, 2015

DOI: 10.1021/jp5116564
J. Phys. Chem. C 2015, 119, 2871−2878

with molecular structures still keeping stable. Owing to these, the organic molecules have some advantages in surface doping. For emerging nanomaterials such as carbon nanotubes,[21] graphene, boron nitride nanotubes,[22,23] hexagonal boron nitride nanosheeets,[24] MoS_2,[25] and so on, tremendous theoretical and experimental efforts have been devoted to study the interactions of these nanomaterials with different organic molecules. To our best knowledge, there is no theoretical or experimental report on the noncovalent surface doping via the organic molecules on phosphorene. Here, by employing the first-principles calculations, we carry out a systematic study to explore the interactions between the single-layer phosphorene and two typical organic molecules with aim of realizing effective n- and p-doping of phosphorene. As we know, a typical p-type dopant should have empty states close to valence band edge (VBE), and on the contrary, a typical n-type dopant should have filled states close to conduction band edge (CBE). In this paper two kinds of organic molecules are used to dope the single-layer phosphorene: one is electrophilic molecule TCNQ possessing effective electron-withdrawing capabilities with an adiabatic electron affinity (EA) of 2.80 eV; the other is nucleophilic molecule TTF possessing effective electron-donating capabilities with an adiabatic ionization potential (IP) of 7.36 eV. Structures of these two molecules are shown in Figures 1a and 1b. Our results indicate that the phosphorene

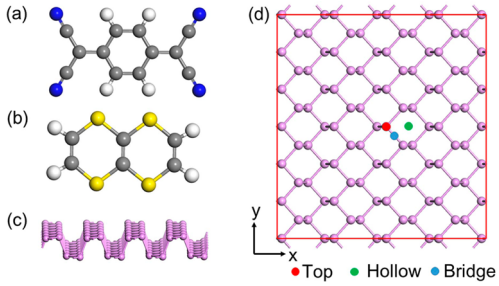

Figure 1. (a) Top view of the molecular structure for TCNQ. (b) Top view of the molecular structure for TTF. (c) Side view for single-layer phosphorene. The C, H, N, and S atoms are represented by gray, white, blue, and yellow balls, respectively. (d) Top view of the 4 × 6 × 1 supercell of phosphorene, with three possible molecular adsorption sites being marked by different colored circles.

becomes a p-type semiconductor after adsorbing the TCNQ molecule as acceptor. On the other hand, after adsorption of the TTF molecule as donor there appear molecule-derived filled states in the band gap of phosphorene, but these states are still far from the CBE. It is also found that if the appropriate external out-of-plane electric field or/and in-plane strain is applied, the effective n-doping of phosphorene will be realized. Moreover, the band gap of the TTF-adsorbed phosphorene can be modulated by the out-of-plane electric field and in-plane strain, making this complex be usable as a variable frequency near- and mid-infrared photoconductive detector.

II. THEORETICAL MODEL AND METHOD

In this study, our first-principles calculations are based on the density functional theory (DFT) implemented in the VASP package.[26] The generalized gradient approximation of Perdew, Burke, and Ernzerhof (GGA-PBE) and projector augmented wave (PAW) potentials are used.[27] In all computations, the kinetic energy cutoff are set to be 520 eV in the plane-wave expansion. The Brillouin zone is sampled with a grid of 3 × 3 × 1 conducted by the Monkhorst−Pack special k-point scheme.[28] All the geometry structures are fully relaxed until energy and forces are converged to 10^{-5} eV and 0.02 eV/Å, respectively. Dipole correction is employed to cancel errors of electrostatic potential, atomic forces, and total energy, caused by periodic boundary condition.[29] The effect of van der Waals (vdW) interaction is accounted for by using empirical correction method proposed by Grimme (DFT-D2),[30] which is a good description of long-range vdW interactions.[31−34] As a benchmark, DFT-D2 calculations give an interlayer distance of 3.25 Å and a binding energy of −25 meV per carbon atom for bilayer graphene, consistent with previous experimental measurements and theoretical studies.[35,36] In order to estimate charge transfer between the organic molecules and phosphorene, we adopt Bader charge analysis method,[37] using the Bader program of Henkelman's group.[38−40]

Unlike a flat structure of graphene, the single-layer phosphorene has a puckered honeycomb structure with each phosphorus atom covalently bonded with three adjacent atoms (Figure 1c). Initial structure of phosphorene used in our simulation is obtained from black phosphorus.[41] Our calculated lattice constants for bulk black phosphorus are a = 3.30 Å, b = 4.56 Å, and c = 11.31 Å, in good agreement with experimental values and other theoretical calculations.[42] The relaxed lattice constants for the single-layer phosphorene are a = 3.30 Å and b = 4.62 Å. To study the adsorption of TCNQ and TTF molecule on the single-layer phosphorene, we adopt a 4 × 6 × 1 supercell containing 96 P atoms, so the molecule−phosphorene adsorption system consists of a 18.49 Å × 19.79 Å × 20.18 Å supercell (Figure 1d). The nearest distance between two adsorbed molecules in adjacent supercells is ∼10 Å, and a large value 15 Å of the vacuum region is used to avoid interaction between two adjacent periodic images. In order to evaluate stability of the molecular adsorption on phosphorene, the adsorption energy is defined as

$$E_a = E_{\text{molecule+phosphorene}} - E_{\text{molecule}} - E_{\text{phosphorene}} \quad (1)$$

where $E_{\text{molecule+phosphorene}}$, E_{molecule}, and $E_{\text{phosphorene}}$ represent total energy of the molecular adsorption on phosphorene, the molecule, and the phosphorene, respectively.

III. RESULTS AND DISCUSSION

To understand how the molecules are adsorbed on phosphorene, we first investigate which adsorption site is the most stable one. Because of highly symmetrical geometries of the TTF and TCNQ molecules, three adsorption sites are considered for each molecule (see Figure 1d): the top of a phosphorus atom (T), the center of a phosphorus hexagon (H), and the center of a phosphorus−phosphorus bond (B). For each of these positions, two molecular orientations are tested, that is to say, long axis of the organic molecules being along the x-direction or y-direction of the unit cell. The adsorbed molecules are initially placed parallel to the phosphorene surface with a vertical distance of 2.7 Å. We have considered various initial configurations for the molecular adsorption on phosphorene, as mentioned above. The adsorption energy for different adsorption configurations after relaxation are shown in Table 1, from which we learned that the adsorption energy difference between different configurations is small.

Next, we make further detailed investigations on only the most stable configurations. The most stable configuration for TCNQ is the top site, with its long axis along the x-direction of

DOI: 10.1021/jp5116564
J. Phys. Chem. C 2015, 119, 2871−2878

Table 1. Adsorption Energies (E_a) of TCNQ and TTF on Phosphorene for Different Adsorption Configurations

system	position	orientation	E_a (eV)
TCNQ/phosphorene	T	*x*	−1.388
		y	−1.368
	H	*x*	−1.142
		y	−0.741
	B	*x*	−1.254
		y	−1.319
TTF/phosphorene	T	*x*	−1.510
		y	−1.283
	H	*x*	−1.510
		y	−1.558
	B	*x*	−1.514
		y	−1.460

unit cell (see Figure 2a). While for TTF, the most stable configuration is the hollow site with its long axis along the *y*-direction of unit cell (see Figure 2b). Here we define equilibrium distance between the molecule and phosphorene as the distance between the nearest atoms of two subsystems. The equilibrium distance between the TCNQ and phosphorene is 3.10 Å; meanwhile, both the TCNQ and phosphorene are slightly crumpled from flat plane due to weak interaction. That is to say, the interaction between the TCNQ molecule and single-layer phosphorene is mainly of physisorption. In comparison with the case of TCNQ, the equilibrium distance between the TTF molecule and single-layer phosphorene is 2.47 Å. The adsorbed TTF molecule is severely bent, and the maximal height difference of the atoms in the molecule reaches 1.14 Å (see Figure 2b). The adsorption of TTF also results in a slight distortion of phosphorene.

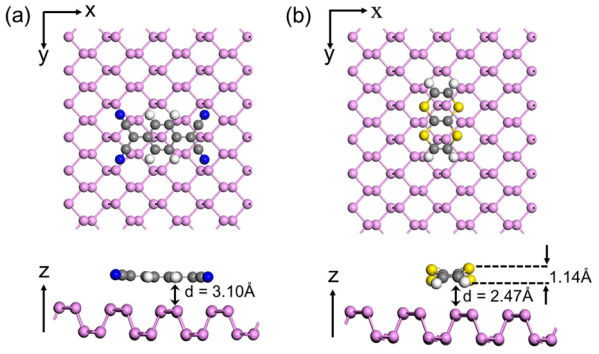

Figure 2. Top and side views of the most stable configurations for the adsorbed (a) TCNQ and (b) TTF molecules on single-layer phosphorene, and the equilibrium distances between the phosphorene and molecules as well as the bending distance of the TTF molecule are also given.

In order to examine how these adsorbed molecules affect the electronic properties of phosphorene, we calculate the electronic band structures of single-layer phosphorene before and after the molecular adsorption. The electronic band structures of pristine phosphorene, TCNQ-adsorbed phosphorene system, and TTF-adsorbed phosphorene system are shown in Figures 3a−c. Clearly, the pristine phosphorene is a direct-gap semiconductor with a band gap of 0.91 eV at Γ point calculated using PBE, in good agreement with previous report.[11] Comparing Figure 3a with Figure 3b, we find that a flat band appears just above the Fermi level (E_F) after the adsorption of TCNQ, and it is mainly derived from the TCNQ molecule (see analysis later in this paper), named as the lowest unoccupied molecular band. However, for the TTF-adsorbed phosphorene system, a flat band which is mainly derived from the TTF molecule (see analysis later in this paper) appears just below the E_F, named as the highest occupied molecular band. It is obvious that these two bands may act as the acceptor state in the TCNQ-adsorbed phosphorene system and the donor state in the TTF-adsorbed phosphorene system, respectively.

The appearances of the acceptor and donor state due to the molecular adsorption reduce the band gap of phosphorene. We define E_p as the new band gap between the lowest unoccupied molecular band and the VBE of phosphorene with TCNQ being adsorbed and E_n as the new band gap between the highest occupied molecular band and the CBE of phosphorene with TTF being adsorbed. A typical p-doped (n-doped) semiconductor requires the enough small E_p (E_n), which means lower activation energy for the holes (electrons) localized at impurity to become charge carriers. For the TCNQ-adsorbed phosphorene system, the lowest unoccupied molecular band (acceptor states) become very close to the phosphorene VBE and E_p is only 0.12 eV, showing that it forms the shallow acceptor states, so a typical p-type doping is realized and there maybe exists considerable charge transfer between the TCNQ molecule and phosphorene. In fact, according to our Bader charge analysis, the charge transfer between them is about 0.35 electron per molecule from

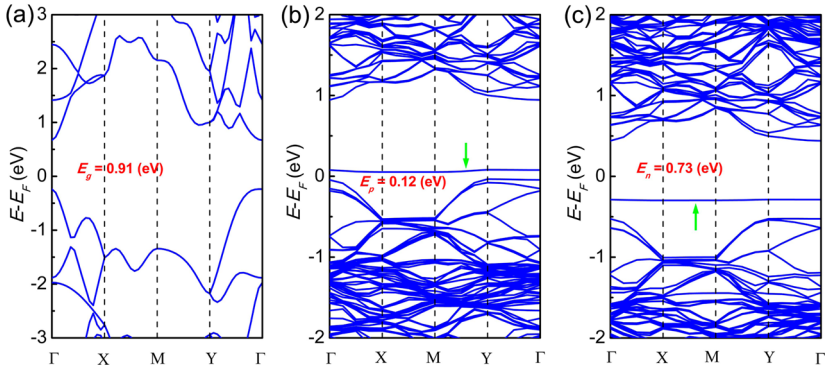

Figure 3. Calculated band structures of (a) pristine phosphorene, (b) TCNQ-adsorbed phosphorene, and (c) TTF-adsorbed phosphorene. The acceptor or donor states from the molecule are indicated by green arrow. Γ (0.0, 0.0, 0.0), X (0.0, 0.5, 0.0), M (0.5, 0.5, 0.0), and Y (0.5, 0.0, 0.0) refer to special points in the first Brillouin zone.

DOI: 10.1021/jp5116564
J. Phys. Chem. C 2015, 119, 2871−2878

phosphorene to TCNQ. Such considerable electron transfer also indicates that the TCNQ-adsorbed phosphorene system is a typical p-type semiconductor. For the TTF-adsorbed phosphorene system, the highest occupied molecular band (donor states) is found to be also close to the phosphorene VBE, not CBE, and E_n reaches 0.73 eV, which is too large to form an effective n-type doping. In fact, it belongs to the case of deep doping and the highest occupied molecular band forms the deep donor states. In addition, Bader charge analysis shows that there is only 0.06 electron per molecule transferring from TTF to phosphorene. Such small charge transfer also suggests that the TTF-adsorbed phosphorene system is not a typical n-type semiconductor.

In order to validate the above conclusions about the doping of phosphorene, we calculate density of states (DOS) for the TCNQ/TTF-adsorbed phosphorene systems and the projected density of states (PDOS) for phosphorene and TCNQ/TTF in two adsorption systems (Figure 4). As shown in Figure 4a, for

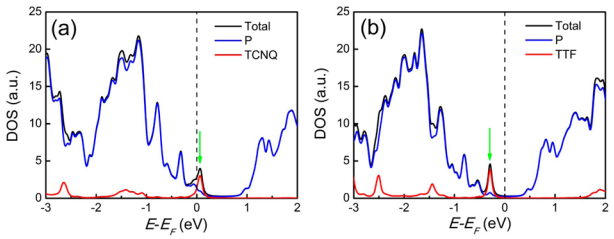

Figure 4. Total DOS and PDOS of the molecule and phosphorene for (a) the TCNQ-adsorbed and (b) TTF-adsorbed phosphorene systems. The dashed line indicates the E_F. The acceptor or donor states from the molecule are indicated by green arrow.

the TCNQ-adsorbed phosphorene system, the introduced new state above the E_F, which is very close to the VBE of phosphorene, is indeed mainly ascribed to the TCNQ molecule. And for the TTF-adsorbed phosphorene system, a new state is introduced below the E_F, far away from the CBE of phosphorene, and it is the TTF molecule that provides the main contribution to this state (see Figure 4b). These results are consistent with the above conclusions that the TCNQ-adsorbed phosphorene system is an effective p-type semiconductor, and the TTF-adsorbed phosphorene system is not an effective n-type semiconductor.

In order to realize the effective n-doping of phosphorene and obtain a typical n-type semiconducting phosphorene, we have also tried to employ the other two typical nucleophilic molecules, i.e., tetrakis(dimethylamino)ethylene (TDAE) and anthracene (ANTR) with adiabatic IPs of 5.36 and 6.40 eV, respectively, as the dopant of single-layer phosphorene. But our calculation results show that the obtained band gap E_n when using the TDAE or ANTR molecule as the dopant is even larger than that in the case of TTF-adsorbed phosphorene system. So, next we try to explore possible modulation of the band structure of the TTF-adsorbed phosphorene by a varied external electric field or strain, which may be helpful to realize the effective n-doping of phosphorene.

Previous studies had showed that the external electric field may affect the charge transfer and energy level alignment between the adsorbed species and substrate,[22,43,44] so we expect that the TTF-adsorbed phosphorene can turn to a typical n-type semiconductor under an appropriate external electric field. The electric field is applied perpendicular to the phosphorene surface, with a strength ranging from −0.5 to 0.5 V/Å. Here we define the positive electric field as the one pointing downward

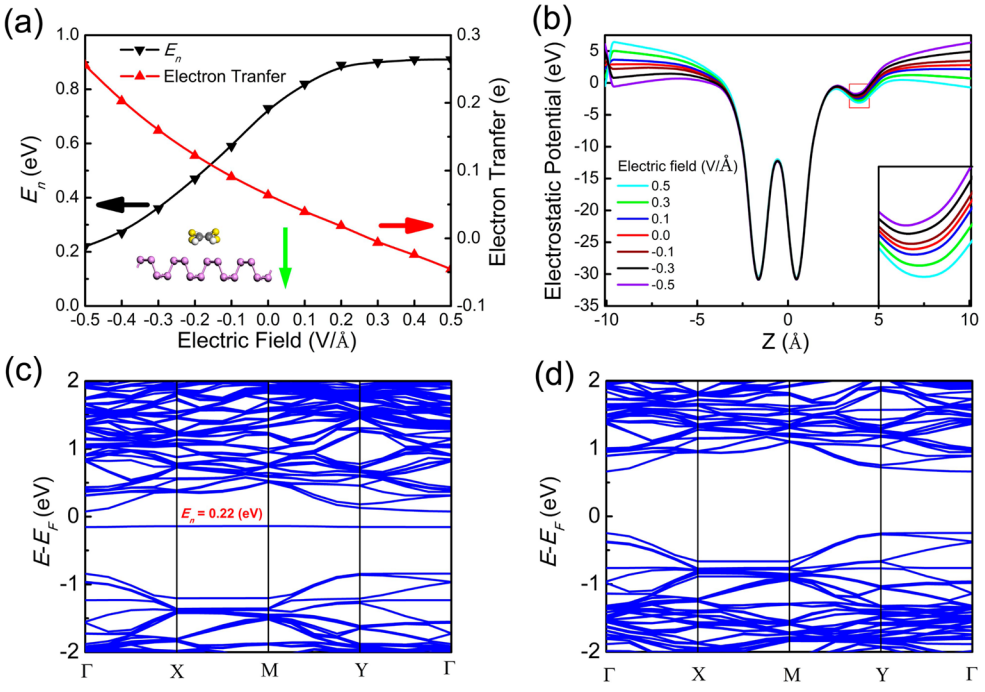

Figure 5. (a) Variations of E_n and TTF-phosphorene electron transfer of the TTF-adsorbed phosphorene system under the external field, and the positive direction of electric field is denoted by the green arrow in the inset. (b) *xy*-averaged electrostatic potential profiles of the TTF-adsorbed phosphorene system under different external electric fields. The magnified potential profile around the TTF molecule are shown in the inset. Band structures of the TTF-adsorbed phosphorene system under the electric fields of (c) −0.5 V/Å and (d) 0.5 V/Å. Γ (0.0, 0.0, 0.0), X (0.0, 0.5, 0.0), M (0.5, 0.5, 0.0), and Y (0.5, 0.0, 0.0) refer to special points in the first Brillouin zone.

DOI: 10.1021/jp5116564
J. Phys. Chem. C 2015, 119, 2871−2878

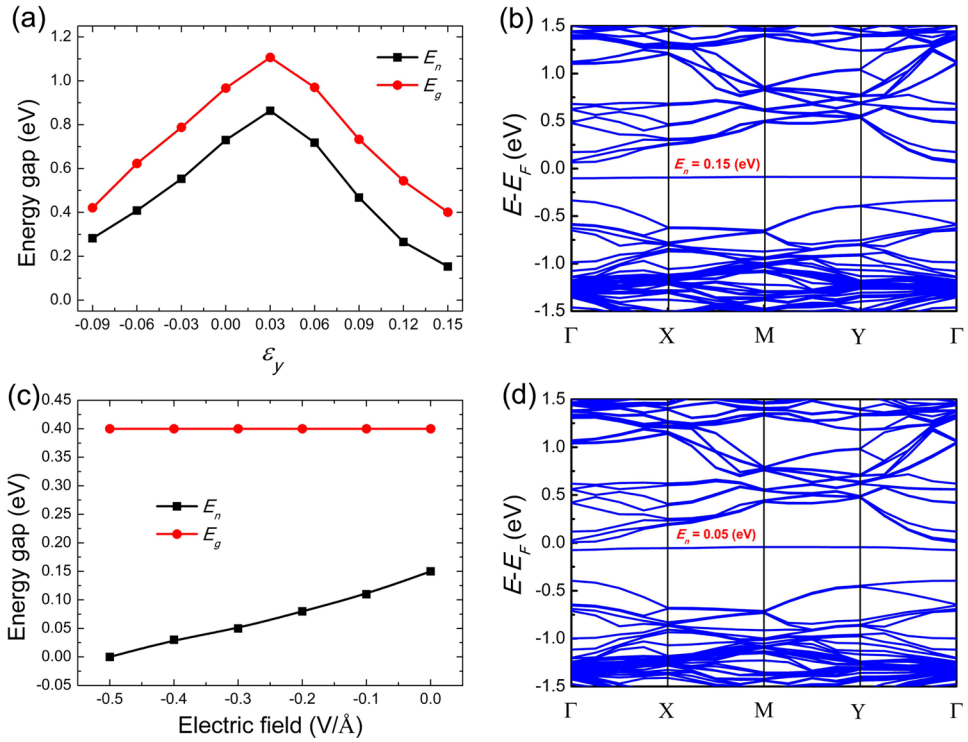

Figure 6. (a) Variations of E_n and E_g of the TTF-adsorbed phosphorene system under the in-plane uniaxial strain along the *y*-direction ε_y. (b) Band structure of the TTF-adsorbed phosphorene system under the uniaxial strain ε_y of 15%. (c) Variations of E_n and E_g of the TTF-adsorbed phosphorene system under the fixed uniaxial strain ε_y of 15% and the negative electric field. (d) Band structure of the TTF-adsorbed phosphorene system under the uniaxial strain ε_y of 15% and the electric field of −0.3 V/Å. Γ (0.0, 0.0, 0.0), X (0.0, 0.5, 0.0), M (0.5, 0.5, 0.0), and Y (0.5, 0.0, 0.0) refer to special points in the first Brillouin zone.

to the phosphorene surface (see red arrow in Figure 5a). As illustrated in Figure 5a, E_n of the TTF-adsorbed phosphorene system varies from 0.22 eV under the electric field of −0.5 V/Å to 0.91 eV under the electric field of 0.5 V/Å based on our PBE calculation, showing a fine controllability. It is observed the highest occupied molecular band moves close to the phosphorene CBE under a negative electric field. Especially, this band becomes the shallow donor state and the TTF-adsorbed phosphorene system is converted to a typical n-type semiconductor under the electric field of −0.5 V/Å. On the other hand, the highest occupied molecular band gets close to and even merges into the phosphorene VBE with increasing electric field. The band structures of the TTF-adsorbed phosphorene system under the electric fields of −0.5 and 0.5 V/Å are plotted in Figures 5c and 5d, respectively. It is noted that in this case properties of the bands derived from the phosphorene do not change obviously with the varied electric field from −0.5 to 0.5 V/Å. In fact, the dependence of band structure of a pristine phospherene on the electric field varying in the same range is also weak according to a recent report[45] and our test (not shown). We have also calculated the charge transfers between the TTF molecule and single-layer phosphorene under different electric fields (also see Figure 5a). Applying the negative electric field is found to enhance the charge transfer. When the field reaches −0.5 V/Å, there is about 0.26 electron transferring from the TTF molecule to single-layer phosphorene, also suggesting the effective n-doping of phosphorene.

This modulation of band structure of the TTF-adsorbed phosphorene system under the external electric field can be understood by examining its electrostatic potential profile. The *xy*-averaged electrostatic potentials of this system under different external electric fields are plotted in Figure 5b. It is revealed that the electrostatic potential below the phosphorene surface increases with increasing electric field, but the electrostatic potential of TTF decreases as the electric field increases, so the electric potential difference between them increase when the electric field changes from the negative to positive. Obviously, if we apply a negative electric field on the TTF-adsorbed phosphorene surface, the electrons transfer more easily from TTF to phosphorene due to the increased electrostatic potential difference of TTF relative to phosphorene, i.e., better electron donation to phosphorene. At the same time, this increase of the electrostatic potential difference also suggests that the highest occupied molecular band will move upward relative to the CBE of phosphorene and then change from the deep donor states to the shallow donor states. So the TTF-adsorbed phosphorene is converted to an effectively n-doped semiconductor under an appropriate negative external electric field.

The good response of the energy position of the TTF-derived donor state in the gap of single-layer phosphorene to the external electric field is related to the specific TTF−phosphorene interaction. If this interaction is too strong, there may occur considerable hybridization between the molecular orbitals of TTF and phosphorene states which will obviously weaken the potential difference between TTF and phosphorene and its induced response to the electric field. But the too weak TTF−phosphorene interaction cannot stabilize the molecule on substrate and will make a negative impact on actual applications. Our calculation for the TTF-adsorbed phosphorene system presents the adsorption energy of up to 1.558 eV, a

DOI: 10.1021/jp5116564
J. Phys. Chem. C 2015, 119, 2871−2878

moderate interaction which avoids the above two disadvantageous statuses.

The external strain has been also employed as a popular and effective method to modulate the electronic structures and related physical properties of various 2D nanosystems.[46−49] We have attempted to apply three types of strains (biaxial strain, uniaxial strain along the x-direction, and uniaxial strain along the y-direction) ranging from −9% to 15%, which were ensured to be in the range of elastic deformation, to the phosphorene plane. Figure 6a shows the calculated band gap E_n of the TTF-adsorbed phosphorene under different in-plane uniaxial strain ε_y along the y-direction. It is found that the band gap E_n can be also modulated effectively by the uniaxial strain ε_y: E_n has the maximum 0.86 eV at the ε_y of about 3% and decreases when the ε_y is far from 3%, reaching 0.28 eV under the compressive strain ε_y = −9% and 0.15 eV under the tensile strain ε_y = 15%. Figure 6b presents the band structure of the TTF-adsorbed phosphorene under the uniaxial tensile strain ε_y of 15%. One can find that when ε_y = 15%, the TTF-derived donor state moves close to the phosphorene CBE with the band gap E_n of 0.15 eV, suggesting the shallow donor states and n-type doping of phosphorene. The uniaxial strain along the x-direction and biaxial strain also bring similar effects, but their resulted E_n are larger than that induced by the uniaxial strain along the y-direction under the same strain intensity (not shown). This modulation of the energy gap E_n by the strain can be interpreted as follows: the phosphorene CBE moves up with decreasing compressive strain and increasing tensile strain before it reaches a maximum because the p_z-derived σ^* state which contributes to the phosphorene CBE is lifted, but beyond this maximum the phosphorene CBE shifts down with increasing tensile strain since the lowered p_x (p_y)-derived π^* states begin to dominate the phosphorene CBE, as revealed in recent studies;[42,45,50] at the same time the highest occupied molecular band of TTF should be relatively stable due to weak influence of substrate strain on the molecular orbitals, so the band gap E_n of the TTF-adsorbed phosphorene system varies along with the lifting or lowering of the phosphorene CBE. In Figure 6a, the energy gaps E_g between the phosphorene CBE and VBE under different strains ε_y are also plotted. It is noted that under the uniaxial tensile strain ε_y of 15%, the energy gap between the TTF-derived donor state and the phosphorene VBE (= $E_g - E_n$) turns to 0.25 eV, which has small difference from the E_n of 0.15 eV, showing that the realized n-doping is not good enough.

In order to realize the good n-doping of the TTF-adsorbed phosphorene system, we try to combine the above two methods, i.e., to apply the out-of-plane electric field and in-plane strain simultaneously. Figure 6c shows the calculated band gaps E_n of the TTF-adsorbed phosphorene and energy gaps E_g between the phosphorene CBE and VBE under a fixed uniaxial strain ε_y = 15% and different negative electric fields. Similar to the case of the TTF-adsorbed phosphorene system without deformation, the negative electric field can decrease the band gap E_n of the deformed TTF-adsorbed phosphorene effectively and even close the band gap under the electric field of −0.5 V/Å. This makes it possible to realize good n-doping of phosphorene. For example, under the electric field of −0.3 V/Å the TTF-derived donor state further moves close to the phosphorene CBE with the band gap E_n of only 0.05 eV, and the energy gap between this donor state and the phosphorene VBE (= $E_g - E_n$) is 0.35 eV at the same time, as shown by the band structure in Figure 6d, so that the good n-doping of phosphorene has been realized. By changing combination of the out-of-plane field intensity and in-plane strain intensity, one will obtain various types of n-doped phosphorene systems with different combinations of the energy gaps between the donor state and the phosphorene VBE/CBE, which may satisfy diversification of industrial application of the phosphorene. Here the combination of two modulation methods with different mechanisms and effects results in realization of the good n-doping of phosphorene under usually accessible conditions.

Besides the potential of the realized effective n-doping in the field of nanoelectonics, our predicted modulation of the band gap of the TTF-adsorbed phosphorene, especially that by the electric field, may be of benefit to the design of infrared photoconductive detector. With the external electric field changing between −0.5 and 0.5 V/Å, the band gap E_n of the TTF-adsorbed phosphorene system varies from 0.22 to 0.91 eV, corresponding to the wavebands of near-infrared and mid-infrared. So, by adjusting the electric field, one can make the TTF-adsorbed phosphorene system absorb infrared light with alterable wavelength and produce the photocurrent, so as to realize a variable-frequency near- and mid-infrared photoconductive detector. Of course, the single-layer phosphorene itself[42,45,50] and the TTF-adsorbed phosphorene (as shown above) also have good response of the band gap to the strain, but in the actual applications the external electric field is easier to be implemented than the strain. And the response of the band gap of single-layer phosphorene to the external electric field is weak in the range of usually accessible field intensity according to a recent report[45] and our test (not shown). Introduction of the TTF molecular adsorbate causes the single-layer phosphorene to have band gap well sensitive to the easily applied external electric field.

It is also worth noting that recent studies showed that the localized midgap states introduced into the semiconductor materials by the adsorption of nanostructure or molecule will open additional relaxation pathways to facilitate the electron transfer upon photoexcitations.[51,52] For example, the photoexcitation and subsequent phonon-assisted intraband relaxation may bring the electron transfer from the carbon nanotube (CNT) to the adsorbed molecule for the system of dinitromethane physisorbed on CNT.[52] In our simulated systems, the TCNQ-derived unoccupied states and TTF-derived occupied states in the gap of phosphorene are likely to play this role. And the phonon-assisted intraband relaxation after photoexcitation will result in the electron transfer from the phosphorene to TCNQ molecule for the TCNQ-adsorbed phosphorene system and from the TTF molecule to phosphorene for the TTF-adsorbed phosphorene system, which can further strengthen the p-type and n-type doping of the single-layer phosphorene, respectively.

IV. SUMMARY

In conclusion, on the basis of DFT calculations, we have performed a theoretical research on the structural and electronic properties of single-layer phosphorene functionalized by the organic molecules. Our calculations show that band gap of the adsorption complexes decreases after the organic molecules are adsorbed because of the impurity states from the molecule. The typical p-type doped phosphorene can be obtained by adsorbing with the typical electrophilic molecule TCNQ which introduces the shallow acceptor states, with considerable electron transfer from phosphorene to TCNQ.

DOI: 10.1021/jp5116564
J. Phys. Chem. C 2015, 119, 2871−2878

While, when the typical nucleophilic molecule TTF is adsorbed on the phosphorene, the introduced donor states are far from the phosphorene CBE so that the adsorption complex does not become effectively n-doped and the corresponding charge transfer is also very small. But when an appropriate external electric field perpendicular to the phosphorene surface with direction from phosphorene to TTF or/and an in-plane unaxial/biaxial strain is applied, the deep donor states will move close to the phosphorene CBE and turn to the shallow ones, so an effectively n-doped phosphorene can be obtained. And the perpendicular electric field and in-plane strain can also modulate the band gap of TTF-adsorbed phosphorene system in the range of near- and mid-infrared wavelength, suggesting potential in the photoconductive detector. Our results suggest the electronic structure of phosphorene can be controlled over a wider range by the adsorption of organic molecules without destroying the phosphorene structural integrity. Thus, it is possible to build phosphorene-based electronic devices by modifying the phosphorene with patterned organic molecules, which may be broaden the applications of phosphorene in the developing nanoelectronics and optoelectronics.

AUTHOR INFORMATION

Corresponding Authors

*E-mail: libin@mail.ustc.edu.cn; Ph: +86-551-63601747; Fax: +86-551-63603748 (B.L.).

*E-mail: jlyang@ustc.edu.cn; Ph: +86-551-63606408; Fax: +86-551-63603748 (J.Y.).

Notes

The authors declare no competing financial interest.

ACKNOWLEDGMENTS

This work is partially supported by the National Key Basic Research Program (2011CB921404), by NSFC (21121003, 91021004, 21233007, 21273210), by CAS (XDB01020300), by Fundamental Research Funds for the Central Universities, and by USTCSCC, SCCAS, Tianjin, and Shanghai Supercomputer Centers.

REFERENCES

(1) Xu, M.; Liang, T.; Shi, M.; Chen, H. Graphene-Like Two-Dimensional Materials. *Chem. Rev.* **2013**, *113*, 3766−3798.

(2) Sun, Z.; Chang, H. Graphene and Graphene-Like Two-Dimensional Materials in Photodetection: Mechanisms and Methodology. *ACS Nano* **2014**, *8*, 4133−4156.

(3) Geim, A. K.; Novoselov, K. S. The Rise of Graphene. *Nat. Mater.* **2007**, *6*, 183−191.

(4) Castro Neto, A. H.; Peres, N. M. R.; Novoselov, K. S.; Geim, A. K. The Electronic Properties of Graphene. *Rev. Mod. Phys.* **2009**, *81*, 109−162.

(5) Vogt, P.; De Padova, P.; Quaresima, C.; Avila, J.; Frantzeskakis, E.; Asensio, M. C.; Resta, A.; Ealet, B.; Le Lay, G. Silicene: Compelling Experimental Evidence for Graphenelike Two-Dimensional Silicon. *Phys. Rev. Lett.* **2012**, *108*, 155501.

(6) Fleurence, A.; Friedlein, R.; Ozaki, T.; Kawai, H.; Wang, Y.; Yamada-Takamura, Y. Experimental Evidence for Epitaxial Silicene on Diboride Thin Films. *Phys. Rev. Lett.* **2012**, *108*, 245501.

(7) Jose, D.; Datta, A. Structures and Chemical Properties of Silicene: Unlike Graphene. *Acc. Chem. Res.* **2014**, *47* (2), 593−602.

(8) Jin, C.; Lin, F.; Suenaga, K.; Iijima, S. Fabrication of a Freestanding Boron Nitride Single Layer and Its Defect Assignments. *Phys. Rev. Lett.* **2009**, *102*, 195505.

(9) Lee, C.; Li, Q.; Kalb, W.; Liu, X. Z.; Berger, H.; Carpick, R. W.; Hone, J. Frictional Characteristics of Atomically Thin Sheets. *Science* **2010**, *328* (5974), 76−80.

(10) Lei, W.; Portehault, D.; Liu, D.; Qin, S.; Chen, Y. Porous Boron Nitride Nanosheets for Effective Water Cleaning. *Nat. Commun.* **2013**, *4*, 1777.

(11) Wang, Q. H.; Kalantar-Zadeh, K.; Kis, A.; Coleman, J. N.; Strano, M. S. Electronics and Optoelectronics of Two-Dimensional Transition Metal Dichalcogenides. *Nat. Nanotechnol.* **2012**, *7*, 699−712.

(12) Li, L.; Yu, Y.; Ye, G. J.; Ge, Q.; Ou, X.; Wu, H.; Feng, D.; Chen, X. H.; Zhang, Y. Black Phosphorus Field-Effect Transistors. *Nat. Nanotechnol.* **2014**, *9*, 372−377.

(13) Liu, H.; Neal, A. T.; Zhu, Z.; Luo, Z.; Xu, X.; Tománek, D.; Ye, P. D. Phosphorene: An Unexplored 2D Semiconductor with a High Hole Mobility. *ACS Nano* **2014**, *8*, 4033−4041.

(14) Qiao, J.; Kong, X.; Hu, Z. X.; Yang, F.; Ji, W. High-Mobility Transport Anisotropy and Linear Dichroism in Few-Layer Black Phosphorus. *Nat. Commun.* **2014**, *5*, 4475.

(15) Xia, F.; Wang, H.; Jia, Y. Rediscovering Black Phosphorus as an Anisotropic Layered Material for Optoelectronics and Electronics. *Nat. Commun.* **2014**, *5*, 4458.

(16) Fei, R.; Yang, L. Strain-Engineering the Anisotropic Electrical Conductance of Few-Layer Black Phosphorus. *Nano Lett.* **2014**, *14*, 2884−2889.

(17) Dai, J.; Zeng, X. C. Bilayer Phosphorene: Effect of Stacking Order on Bandgap and Its Potential Applications in Thin-Film Solar Cells. *J. Phys. Chem. Lett.* **2014**, *5*, 1289−1293.

(18) Guo, H.; Lu, N.; Dai, J.; Wu, X.; Zeng, X. C. Phosphorene Nanoribbons, Phosphorus Nanotubes, and van der Waals Multilayers. *J. Phys. Chem. C* **2014**, *118*, 14051−14059.

(19) Deng, Y.; Luo, Z.; Conrad, N. J.; Liu, H. Black Phosphorus-Monolayer MoS_2 van der Waals Heterojunction p-n Diode. *ACS Nano* **2014**, *8*, 8292−8299.

(20) Liu, Y.; Xu, F.; Zhang, Z.; Penev, E. S.; Yakobson, B. I. Two-Dimensional Mono-Elemental Semiconductor with Electronically Inactive Defects: the Case of Phosphorus. *Nano Lett.* **2014**, *14*, 6782−6786.

(21) Takenobu, T.; Takano, T.; Shiraishi, M.; Murakami, Y.; Ata, M.; Kataura, H.; Achiba, Y.; Iwasa, Y. Stable and Controlled Amphoteric Doping by Encapsulation of Organic Molecules inside Carbon Nanotubes. *Nat. Mater.* **2003**, *2*, 683−688.

(22) He, W.; Li, Z.; Yang, J.; Hou, J. G. Electronic Structures of Organic Molecule Encapsulated BN Nanotubes under Transverse Electric Field. *J. Chem. Phys.* **2008**, *129*, 024710.

(23) He, W.; Li, Z.; Yang, J.; Hou, J. G. A First Principles Study on Organic Molecule Encapsulated Boron Nitride Nanotubes. *J. Chem. Phys.* **2008**, *128*, 164701.

(24) Tang, Q.; Zhou, Z.; Chen, Z. Molecular Charge Transfer: A Simple and Effective Route to Engineer the Band Structures of BN Nanosheets and Nanoribbons. *J. Phys. Chem. C* **2011**, *115*, 18531−18537.

(25) Mouri, S.; Miyauchi, Y.; Matsuda, K. Tunable Photoluminescence of Monolayer MoS_2 via Chemical Doping. *Nano Lett.* **2013**, *13*, 5944−5948.

(26) Kresse, G.; Hafner, J. Ab Initio Molecular Dynamics for Liquid Metals. *Phys. Rev. B* **1993**, *47*, 558−561.

(27) Perdew, J. P.; Burke, K.; Ernzerhof, M. Generalized Gradient Approximation Made Simple. *Phys. Rev. Lett.* **1996**, *77*, 3865−3868.

(28) Monkhorst, H. J.; Pack, J. D. Special Points for Brillouin-Zone Integrations. *Phys. Rev. B* **1976**, *13*, 5188−5192.

(29) Makov, G.; Payne, M. Periodic Boundary Conditions in Ab Initio Calculations. *Phys. Rev. B* **1995**, *51*, 4014−4022.

(30) Grimme, S. Semiempirical GGA-Type Density Functional Constructed with a Long-Range Dispersion Correction. *J. Comput. Chem.* **2006**, *27*, 1787−1799.

(31) Grimme, S.; Mu, C.; Antony, J. Noncovalent Interactions between Graphene Sheets and in Multishell (Hyper)Fullerenes. *J. Phys. Chem. C* **2007**, *111*, 11199−11207.

(32) Yuan, L.; Li, Z.; Yang, J. Hydrogenated Bilayer Wurtzite SiC Nanofilms: A Two-Dimensional Bipolar Magnetic Semiconductor Material. *Phys. Chem. Chem. Phys.* **2013**, *15* (2), 497−503.

DOI: 10.1021/jp5116564
J. Phys. Chem. C 2015, 119, 2871−2878

(33) Hu, W.; Xia, N.; Wu, X.; Li, Z.; Yang, J. Silicene as a Highly Sensitive Molecule Sensor for NH_3, NO and NO_2. *Phys. Chem. Chem. Phys.* **2014**, *16*, 6957−6962.
(34) Hu, W.; Li, Z.; Yang, J. Electronic and Optical Properties of Graphene and Graphitic ZnO Nanocomposite Structures. *J. Chem. Phys.* **2013**, *138*, 124706.
(35) Baskin, Y.; Meyer, L. Lattice Constants of Graphite at Low Temperatures. *Phys. Rev.* **1955**, *100*, 544−544.
(36) Zacharia, R.; Ulbricht, H.; Hertel, T. Interlayer Cohesive Energy of Graphite from Thermal Desorption of Polyaromatic Hydrocarbons. *Phys. Rev. B* **2004**, *69*, 155406.
(37) Bader, R. F. W. *Atoms in Molecules - A Quantum Theory*; Oxford University Press: Oxford, UK, 1990.
(38) Henkelman, G.; Arnaldsson, A.; Jónsson, H. A Fast and Robust Algorithm for Bader Decomposition of Charge Density. *Comput. Mater. Sci.* **2006**, *36*, 354−360.
(39) Sanville, E.; Kenny, S. D.; Smith, R.; Henkelman, G. Improved Grid-Based Algorithm for Bader Charge Allocation. *J. Comput. Chem.* **2007**, *28*, 899−908.
(40) Tang, W.; Sanville, E.; Henkelman, G. A Grid-Based Bader Analysis Algorithm without Lattice Bias. *J. Phys.: Condens. Matter* **2009**, *21*, 084204.
(41) Brown, A.; Rundqvist, S. Refinement of the Crystal Structure of Black Phosphorus. *Acta Crystallogr.* **1965**, *19*, 684−685.
(42) Peng, X.; Wei, Q.; Copple, A. Strain-Engineered Direct-Indirect Band Gap Transition and Its Mechanism in Two-Dimensional Phosphorene. *Phys. Rev. B* **2014**, *90*, 085402.
(43) Tang, S.; Cao, Z. Defect-Induced Chemisorption of Nitrogen Oxides on (10,0) Single-Walled Carbon Nanotubes: Insights from Density Functional Calculations. *J. Chem. Phys.* **2009**, *131*, 114706.
(44) Tang, S.; Cao, Z. Adsorption of Nitrogen Oxides on Graphene and Graphene Oxides: Insights from Density Functional Calculations. *J. Chem. Phys.* **2011**, *134*, 044710.
(45) Li, Y.; Yang, S.; Li, J. Modulation of the Electronic Properties of Ultrathin Black Phosphorus by Strain and Electrical Field. *J. Phys. Chem. C* **2014**, *118*, 23970−23976.
(46) Conley, H. J.; Wang, B.; Ziegler, J. I.; Haglund, R. F., Jr.; Pantelides, S. T.; Bolotin, K. I. Bandgap Engineering of Strained Monolayer and Bilayer MoS_2. *Nano Lett.* **2013**, *13*, 3626−3630.
(47) Yun, W. S.; Han, S. W.; Hong, S. C.; Kim, I. G.; Lee, J. D. Thickness and Strain Effects on Electronic Structures of Transition Metal Dichalcogenides: 2H-MX_2 Semiconductors (M = Mo, W; X = S, Se, Te). *Phys. Rev. B* **2012**, *85*, 033305.
(48) Guo, H.; Lu, N.; Wang, L.; Wu, X.; Zeng, X. C. Tuning Electronic and Magnetic Properties of Early Transition-Metal Dichalcogenides via Tensile Strain. *J. Phys. Chem. C* **2014**, *118*, 7242−7249.
(49) Hui, Y. Y.; Liu, X.; Jie, W.; Chan, N. Y.; Hao, J.; Hsu, Y.-T.; Li, L.-J.; Guo, W.; Lau, S. P. Exceptional Tunability of Band Energy in a Compressively Strained Trilayer MoS_2 Sheet. *ACS Nano* **2013**, *7*, 7126−7131.
(50) Rodin, A. S.; Carvalho, A.; Castro Neto, A. H. Strain-Induced Gap Modification in Black Phosphorus. *Phys. Rev. Lett.* **2014**, *112*, 176801.
(51) Kilin, D. S.; Micha, D. A. Relaxation of Photoexcited Electrons at a Nanostructured Si(111) Surface. *J. Phys. Chem. Lett.* **2010**, *1*, 1073−1077.
(52) Chu, I.-H.; Kilin, D. S.; Cheng, H.-P. First-Principles Studies of Photoinduced Charge Transfer in Noncovalently Functionalized Carbon Nanotubes. *J. Phys. Chem. C* **2013**, *117*, 17909−17918.

DOI: 10.1021/jp5116564
J. Phys. Chem. C 2015, 119, 2871−2878